

Effect of Branching on the Scaling Behavior of Poly(ether amide) Dendrons and Dendrimers

Shan Wong,* Dietmar Appelhans, Brigitte Voit, and Ulrich Scheler

Institut fuer Polymerforschung Dresden e.V.,
Hohe Strasse 6, D-01069 Dresden, Germany

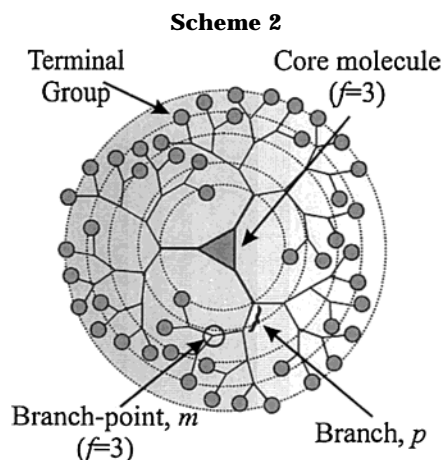
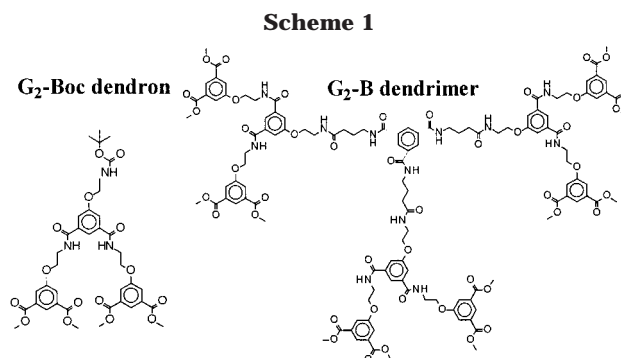
Received September 25, 2000

Introduction. The influence of polymer branching on solution properties has long been of experimental and theoretical interest, as a minor degree of branching can appreciably alter properties such as solubility and viscosity.^{1,2} Polymer branching can occur randomly or regularly. Dendrimers, consisting of a core molecule surrounded by dendrons, are an example of regular branching.^{3–6} The uniform and high degree of branching in dendrimers results in well-defined structures. Theoretical models and computer simulations can predict the structure and explore the density profile within the dendrimer.^{7–10} Experimental studies can determine dendrimer size and the apparent density, typically by scattering techniques, although intrinsic viscosity and pulsed field-gradient nuclear magnetic resonance (PFGNMR) measurements are also used.^{11–15} These studies show that dendrimers have a globular structure, which is not spherical at lower generation but becomes increasingly spherical above the third generation.

The dependence of dendrimer radius on molecular weight follows a power-law relationship. The power-law scaling exponent for dendrimers with a trifunctional core and dendrons is typically found to be about three,^{11,12} which is often interpreted as representative of the dendrimer molecular dimension (i.e., globular) and as evidence for a compact, space-filling nature. The scaling exponent can alternatively be considered in the context of branching, although such an interpretation of experimental results is not common.

In this paper, diffusion rates of trifunctional poly(ether amide) dendrons and dendrimers at low generations are measured by PFGNMR. Examples of a second generation poly(ether amide) dendron and dendrimer are shown in Scheme 1. The hydrodynamic radii are calculated from the diffusion rates using the Stokes–Einstein equation. The relationship between hydrodynamic radius and molecular weight is then used to determine a scaling exponent. An existing statistical branching model^{16,17} is employed to predict the exponent for poly(ether amide) dendrimers. Comparison between the experimentally derived and model-predicted exponents supports the establishment of the scaling exponent as an indicator of dendrimer branching behavior. The model-predicted exponent for tetrafunctional dendrimers provides further evidence for this newly established relationship.

Theoretical branching models for randomly and regularly branched polymers have been developed^{16–18} and are reviewed by Yamakawa.¹⁹ An isotropic branching model which considers only random-flight chains was developed by Kataoka¹⁶ and by Kurata and Fukatsu¹⁷ to predict the unperturbed dimension of the branched



polymer. An isotropically branched polymer consists of a core of f functionality, from which all future branch generations of the same functionality grow in all directions. This type of branching is realized in dendrimers. A two-dimensional representation of a fourth-generation trifunctional dendrimer is shown in Scheme 2 to illustrate and define the terms used here. The model is summarized below.

A branching factor, q , is defined as the ratio of the mean-square statistical radius of a branched polymer $\langle S^2 \rangle_b$ to a linear polymer $\langle S^2 \rangle_l$ as

$$q \equiv \langle S^2 \rangle_b / \langle S^2 \rangle_l \quad (1)$$

In dilute solution, the square root of $\langle S^2 \rangle_l$ is proportional to the radius of gyration $R_{g,l}$.¹⁹ The q -factor for an isotropically branched polymer of identical branch lengths is given by¹⁶

$$q_{\text{iso}} = \frac{3p-2}{p^2} + \frac{6}{p^3} \sum_{\text{all pairs}} p_s \quad (2)$$

where p_s is the number of branches separating any given pair of branches. The sum is taken over all but adjacent branch pairs. The total number of branches p and the number of branch points m are respectively given by¹⁷

$$p = (f-1)m + 1 \quad (3a)$$

$$m = \frac{f(f-1)^k - 2}{f-2} \quad (3b)$$

where k is the generation, and f is the number of

* Corresponding author.

Table 1. ^1H Self-Diffusion Rates and the Calculated Hydrodynamic Radii for Poly(ether amide) Dendrons and Dendrimers; Branching Factors, q_{iso} , for Trifunctional Isotropically branched Polymers Are Calculated for Generations 0–3

| <i>k</i> | MW (g/mol) | sample | D_0 ($\times 10^{-11}$ m ² /s) | R_h (Å) | q_{iso} |
|----------|------------|---------------------|--|-----------|------------------|
| 1 | 381.42 | G ₁ –Boc | 18.7 ± 0.8 | 4.78 | |
| 2 | 795.80 | G ₂ –Boc | 12.2 ± 0.3 | 7.35 | |
| 3 | 1680.60 | G ₃ –Boc | 7.92 ± 0.13 | 11.3 | |
| 0 | 210.14 | G ₀ –A | 17.5 ± 0.5 | 5.11 | 0.778 |
| 0 | 465.46 | G ₀ –B | 12.4 ± 0.2 | 7.21 | (0.778) |
| 1 | 1171.20 | G ₁ –B | 9.34 ± 0.17 | 9.57 | 0.605 |
| 2 | 2498.40 | G ₂ –B | 6.70 ± 0.26 | 13.3 | 0.442 |
| 3 | 5153.00 | G ₃ –B | 5.10 ± 0.23 | 17.5 | 0.305 |
| 0 | 760.02 | G ₀ –C | 9.71 ± 0.21 | 9.22 | (0.778) |
| 1 | 1465.07 | G ₁ –C | 7.91 ± 0.35 | 11.3 | (0.605) |
| 2 | 2793.00 | G ₂ –C | 6.27 ± 0.58 | 14.3 | (0.442) |

branches radiating from the branch point. The radius of gyration of a branched polymer $R_{g,b}$ is then related to that of a linear polymer by $(R_{g,l}q_{\text{iso}}^{0.5})$. $R_{g,l}$ varies as $M^{0.5}$ for a Gaussian chain¹⁹ to give

$$R_{g,b} \propto \sqrt{Mq_{\text{iso}}} \quad (4)$$

The radius of gyration for an isotropically branched polymer of a given functionality and generation can thus be predicted from this statistical model. Small-angle neutron scattering results have indicated that the dendrimer radius of gyration is relatively insensitive to changes in temperature and solvent quality.¹³

Experimental Section. Synthesis and purification of trifunctional poly(ether amide) dendrons and dendrimers have been reported previously.²⁰ Here, the trifunctional core molecules are denoted G₀–A, G₀–B, and G₀–C, where A, B, and C are trimesic acid, 1,3,5-tris[*N*-(3-carboxypropyl)aminocarbonyl]benzene, and 1,3,5-tris[*N*-(10-carboxydecyl)aminocarbonyl]benzene, respectively. The only difference between cores B and C is the alkyl chain length. The dendrons are designated G_{1/2/3}–Boc (t-butoxycarbonyl) and the dendrimers G_{1/2/3}–B and G_{1/2}–C. The numerical subscript refers to the generation. The molecular weights of the dendrons and dendrimers are given in Table 1.

^1H diffusion measurements were carried out in a 7 T superconducting magnet with a Bruker AMX300 spectrometer. The ^1H Larmor frequency was 300.13 MHz. Magnetic field gradients up to 1 T/m were delivered by a microimaging system (Bruker Micro2.5). Gradient strength and linearity were calibrated by imaging an object of known dimension and by measuring the diffusion rate of water. All experiments were conducted at 20 °C. Temperature stability was maintained by a gradient-coil cooling system to within ± 0.2 °C. Polymer samples were dissolved in perdeuterated dimethyl sulfoxide ($\eta_s = 2.4 \times 10^{-3}$ Pa s at 20 °C) in 5 mm NMR tubes.

Dendrimer diffusion rates were measured by spin-echo and stimulated-echo pulse sequences.^{21,22} In these sequences, the interval between two gradient pulses gives the observation time, Δ , over which root-mean-square displacements are measured. These displacements cause a related decay of the NMR signal intensity which is interpreted as a diffusion rate using the Stejskal–Tanner equation,²¹

$$S(g)/S(0) = \exp[-D\gamma^2 g^2 \delta^2 (\Delta - \delta/3)] \quad (5)$$

where γ is the gyromagnetic ratio, D is the one-

dimensional diffusion rate, and g and δ are the gradient strength and duration, respectively. Diffusion rates were obtained from nonlinear regression.

Results and Discussion. Signal decay curves for all dendritic poly(ether amide)s exhibited the following features. The Stejskal–Tanner plots were linear, confirming that the molecular weight was monodisperse.²³ The decay curves were invariant with Δ and gradient direction, confirming that the diffusion was isotropic and time-independent. The self-diffusion rates were determined from integrated intensity of the core-phenyl proton signal and are summarized in Table 1.

The hydrodynamic radius of an incompressible spherical particle of radius R_h moving randomly in a fluid of viscosity η_s can be calculated from the self-diffusion rate using the Stokes–Einstein relationship,

$$D_0 = \frac{k_B T}{6\pi\eta_s R_h} \quad (6)$$

where k_B is the Boltzmann constant and T the temperature. The hydrodynamic radii for the dendritic poly(ether amide)s are given in Table 1, and the relationship between hydrodynamic radius and molecular weight is shown in Figure 1a. The scaling exponents, ν , are given by the inverse slope of the double-logarithmic plot as $R_h \propto M^{1/\nu}$. They are 1.73 ± 0.01 for the dendrons and 2.63 ± 0.08 and 2.98 ± 0.12 for the core B and core C dendrimers, respectively.

The scaling exponent increases from below two for the dendrons to almost three for the dendrimers. The size increase with molecular weight is thus faster for the dendrons. The dendrimer exponent increases slightly with core spacer length (recall the difference between cores B and C is the length of the flexible alkyl chain). The exponents (~ 3) for these dendrimers are consistent with that of trifunctional poly(propylene imine) dendrimers determined from viscosity-derived hydrodynamic radii.¹¹

The model-based scaling exponent for the poly(ether amide) dendrimers is determined from the molecular weight dependence of radius of gyration, which is calculated from eq 4. The use of radius of gyration is justified by the fact that it is related to the hydrodynamic radius by a constant.¹¹ The q_{iso} factors for trifunctional dendrimers calculated from eqs 2 and 3 are shown in Table 1. The double-logarithmic plot of the predicted $R_{g,b}$ as a function of M is shown in Figure 1b. The slope gives an exponent of 2.86 for all trifunctional poly(ether amide) dendrimers. The model-based scaling exponent agrees closely with the experimentally measured exponents.

The fact that a model which was developed from purely statistical branching arguments predicts a scaling exponent similar to the diffusion-based experimental exponents suggests that the type and extent of branching is the key determinant of dendrimer size and density. It may therefore be misleading to relate the scaling exponent only to the dendrimer dimension. This conclusion is further supported by comparing the scaling exponents of tetrafunctional dendrimers. The model predicts an exponent of 5.70. An experimental exponent of 5.72 was determined using the hydrodynamic radii reported for tetrafunctional carboxyl-terminated cascade dendrimers by Zhang and co-workers.²⁴ ($k = 2-4$ at 0.1 degree of ionization in 0.1 M NaCl). The model-based and experimental-based exponents for these tetrafunc-

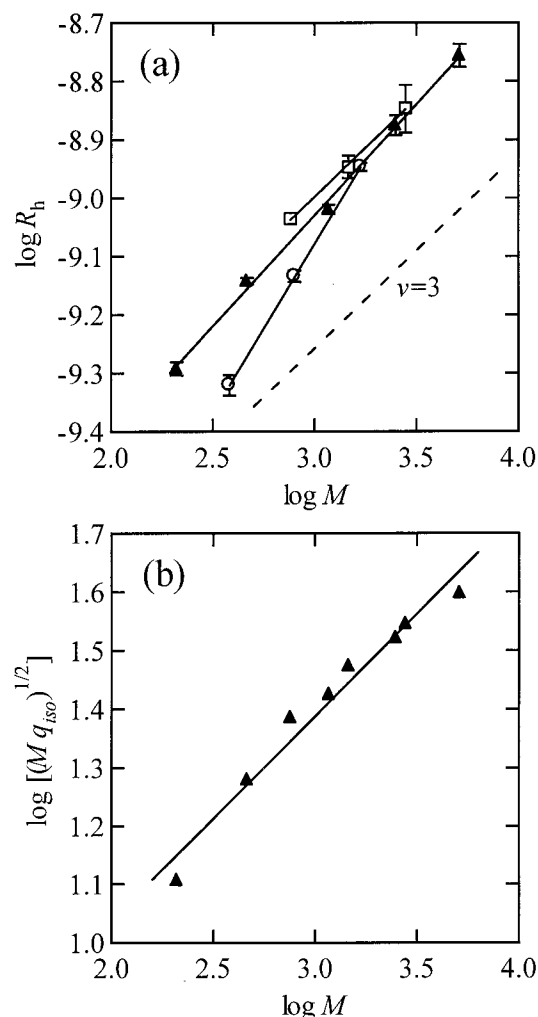


Figure 1. (a) Scaling of hydrodynamic radius to molecular weight for the dendritic poly(ether amide) dendrons and dendrimers. The slopes are 0.579 ± 0.003 for G_{1/2/3}-Boc (○), 0.380 ± 0.011 for core B (▲), and 0.336 ± 0.014 for core C (□) dendrimers. The dotted line represents a scaling exponent of 3. (b) Scaling between the model-predicted radii and molecular weights of the dendrimers. The slope is 0.35 ± 0.03 .

tional dendrimers both exceed the Euclidean dimension. Incidentally, in this case, the experimentally based exponent decreases with increasing degree of ionization, as the electrostatic repulsion between chain end groups exert an additional influence on the dendrimer size.

Conclusions. The self-diffusion rates of trifunctional poly(ether amide) dendrons and dendrimers were measured by PFGNMR and the hydrodynamic radii calculated from the Stokes–Einstein equation. The relationship between hydrodynamic radius and molecular weight

gave a scaling exponent of 1.73 for the dendrons and exponents close to the Euclidean dimension of three for the dendrimers. The scaling exponent derived from a random-flight isotropic branching model for these dendrimers agreed well with the exponents determined from diffusion measurements. The agreement supports the establishment of the exponent as an indicator of the dendrimer branching behavior. This interpretation is further supported by the agreement between the theoretical and experimental exponents for tetrafunctional dendrimers.

Acknowledgment. This work is supported by the Deutsche Forschungsgemeinschaft (DFG) under Grants SCHE 524-1/3 and SCHE 524-2/1.

References and Notes

- (1) Flory, P. J. *Principles in Polymer Chemistry*; Cornell University Press: Ithaca, NY, 1953.
- (2) Burchard, W. *Adv. Polym. Sci.* **1999**, *143*, 113.
- (3) Tomalia, D. A.; Naylor, A. M.; Goddard, A. M. *Angew. Chem.* **1990**, *102*, 119.
- (4) Newkome, G. R.; Moorefield, C. N.; Vögtle, F. *Dendritic Molecules-Concepts, Syntheses, Perspective*; VCH: Weinheim, 1996.
- (5) Bosman, A. W.; Janssen, H. M.; Meijer, E. W. *Chem. Rev.* **1999**, *99*, 1665.
- (6) Fréchet, J. M. J.; Hawker, C. J. In *Comprehensive Polymer Science*, 2nd Suppl.; Aggarwal, S. L., Russo, S., Eds.; Elsevier: Oxford, 1996.
- (7) de Gennes, P. G.; Hervet, H. *J. Phys., Lett.* **1983**, *44*, L351.
- (8) Lescanec, R. L.; Muthukumar, M. *Macromolecules* **1990**, *23*, 2280.
- (9) Mansfield, M. L.; Klushin, L. I. *Macromolecules* **1993**, *26*, 4262.
- (10) Murat, M.; Grest, G. S. *Macromolecules* **1996**, *29*, 1278.
- (11) Scherrenberg, R.; Coussens, B.; van Vliet, P.; Edouard, G.; Brackman, J.; de Brabander, E.; Mortensen, K. *Macromolecules* **1998**, *31*, 456.
- (12) Prosa, T. J.; Bauer, B. J.; Amis, E. J.; Tomalia, D. A.; Scherrenberg, R. *J. Polym. Sci., Part B* **1997**, *35*, 2913.
- (13) Topp, A.; Bauer, B. J.; Tomalia, D. A.; Amis, E. J. *Macromolecules* **1999**, *32*, 7232.
- (14) Young, J. K.; Baker, G. R.; Newkome, G. R.; Morris, K. F.; Johnson, J. C. S. *Macromolecules* **1994**, *27*, 3464.
- (15) Ihre, H.; Hult, A.; Soderlind, E. *J. Am. Chem. Soc.* **1996**, *118*, 6388.
- (16) Kataoka, S. *Busseiron-Kenkyu* **1953**, *66*, 102.
- (17) Kurata, M.; Fukatsu, M. *J. Chem. Phys.* **1964**, *41*, 2934.
- (18) Zimm, B. H.; Stockmayer, W. H. *J. Chem. Phys.* **1949**, *17*, 1301.
- (19) Yamakawa, H. *Modern Theory of Polymer Solutions*; Harper & Row: New York, 1971; Chapter 2.
- (20) Appelhans, D.; Komber, H.; Voigt, D.; Haussler, L.; Voit, B. I. *Macromolecules* **2000**, *33*, 9494.
- (21) Stejskal, E. O.; Tanner, J. E. *J. Chem. Phys.* **1965**, *42*, 288.
- (22) Stejskal, E. O. *J. Chem. Phys.* **1965**, *43*, 3597.
- (23) von Meerwall, E. D. *J. Magn. Reson.* **1982**, *50*, 409.
- (24) Zhang, H.; Dubin, P. L.; Kaplan, J.; Moorefield, C. N.; Newkome, G. R. *J. Phys. Chem. B* **1997**, *101*, 3494.

MA001644U